Plant Gene 27 (2021) 100313

Contents lists available at ScienceDirect

Plant Gene

journal homepage: www.elsevier.com/locate/plantgene

Genome-wide investigation of *SQUAMOSA* promoter binding protein-like transcription factor family in pearl millet (*Pennisetum glaucum* (L) R. Br.)

Pei Yu [a], Harshraj Shinde [b], Ambika Dudhate [c], Daisuke Tsugama [a], Shashi Kumar Gupta [d], Shenkui Liu [e], Tetsuo Takano [a,*]

[a] Asian Natural Environmental Science Center (ANESC), The University of Tokyo, Nishitokyo-shi, Tokyo, Japan
[b] Environmental Epigenetics and Genetics Group, Department of Horticulture, College of Agriculture, Food and Environment, University of Kentucky, Lexington, KY, USA
[c] Department of Pharmaceutical Sciences, Center for Pharmaceutical Research and Innovation, College of Pharmacy, University of Kentucky, Lexington, KY, USA
[d] International Crops Research Institute for the Semi-Arid Tropics (ICRISAT), Hyderabad, Telangana State, India
[e] State Key Laboratory of Subtropical Silviculture, Zhejiang A and F University, Lin'an, Hangzhou, China

ARTICLE INFO

Keywords:
Pearl millet
SBP genes
Transcription factor
microRNA
Abiotic stress

ABSTRACT

Abiotic stress negatively affects the yield of many crops. The *SQUAMOSA* promoter binding protein-like proteins (SBPs) represent a family of plant-specific transcription factors which play essential roles in plant growth, development, and stress responsiveness. In this study, 18 putative *SBP*s (*PgSBP*s) were identified in the genome of pearl millet on the basis of the SBP domain. One or two zinc finger-like structure(s) and a nuclear localization signal (NLS) were found in the SBP domains of all the PgSBPs. Fourteen *PgSBP*s were distributed on 7 chromosomes unevenly, while the other 4 were located on the scaffolds (i.e., non-chromosomal genomic sequences). Moreover, all the *PgSBP*s were clustered into seven groups (I-VII) based on the phylogenetic analysis. The intron/exon structures and the motif composition were similar between *PgSBP*s within the same groups. *PgSBP*s in groups V and VII were predicted as the targets of two microRNAs, *PgmiR156q* and *PgmiR529b*. Some *PgSBP*s have abscisic acid (ABA)-responsive elements and stress-responsive elements in their promoters. Expression levels of these *PgSBP*s were upregulated by abiotic stresses and downregulated by ABA. Together, this study shows a comprehensive overview of *PgSBP*s and provides vital information for elucidating the biological functions of *PgSBP*s.

1. Introduction

Plant growth is adversely affected by various abiotic stresses including drought, salinity, heat, and cold. Plants often establish physiological and metabolic defense systems to respond to these adverse conditions. In higher plants, transcription factors (TFs) play vital roles in the regulating physiological processes and adapting to environmental stresses through various signal transduction pathways (Chen and Rajewsky, 2007). *SQUAMOSA* promoter binding protein-like protein (SBP or SPL) genes encode a plant-specific family of TFs, which have a highly conserved SBP domain with approximately 76 amino acid residues. This conserved domain consists of two zinc-finger structures (Zn-1 and Zn-2) and a nuclear localization signal (NLS) (Yamasaki et al., 2004). Two *SBP* genes were first identified in *Antirrhinum majus* with the ability for binding the promoter region of the floral meristem identity gene *SQUAMOSA* (Klein et al., 1996). *SBP* genes also play important roles in the regulation of plant architecture (Jiao et al., 2010), the vegetative phase change (Wang et al., 2009), anthocyanin biosynthesis (Gou et al., 2011), gibberellin (GA) biosynthesis and signaling (Yu et al., 2012), and stress responses (Cui et al., 2014).

MicroRNAs, non-coding 20–24 nucleotides small RNAs, induce either transcript cleavage or transcription repression (Chen, 2009). Many *SBP* genes are targeted by a microRNA, *miR156*. In Arabidopsis, this *miR156/SBP* module regulates root development (Cui et al., 2014) and affects secondary metabolite accumulation, which can improve stress tolerance (Yu et al., 2015). In rice, *OsSPL14*, which is regulated by *OsmiR156*, improves panicle branching, grain yield, and shoot branching (Jiao et al., 2010; Miura et al., 2010). In switchgrass, the

Abbreviations: SBP, SQUAMOSA promoter binding protein-like protein; NLS, nuclear location signal; ML, maximum-likelihood; MW, molecular weight; pI, isoelectric point; qRT-PCR, quantitative reverse transcription-PCR; ABA, abscisic acid; GA, gibberellic acid; ROS, reactive oxygen species.

* Corresponding author.
E-mail address: takano@anesc.u-tokyo.ac.jp (T. Takano).

https://doi.org/10.1016/j.plgene.2021.100313
Received 17 March 2021; Received in revised form 1 June 2021; Accepted 11 June 2021
Available online 15 June 2021

overexpression of *miR156* induces aerial bud formation, while the overexpression of *SPL4* suppresses bud formation and tillering (Gou et al., 2017). In alfalfa, *miR156* improves drought and heat stress tolerance by silencing *SPL13* (Arshad et al., 2017; Matthews et al., 2019). Another microRNA, *miR529*, sharing 14–16 nucleotides with *miR156*, was also reported to target *SBP*s in plants (Zhang and Ling, 2018).

Pearl millet (*Pennisetum glaucum* (L.) R. Br., syn. *Cenchrus americanus* (L.) Morrone), is a highly cross-pollinated diploid ($2n = 2x = 14$) with a draft genome size of 1.79 Gb (Varshney et al., 2017). It is a C4 cereal crop with nutrient-rich seeds and can grow in marginal environments characterized by low and/or unstable rainfall, poor soil conditions, and high temperature. Although the roles of SBP genes have been revealed in many plants, such as Arabidopsis (Cardon et al., 1999), rice (Xie et al., 2006), cotton (Zhang et al., 2014), foxtail millet (Bennetzen et al., 2012), pepper (Zhang et al., 2016), tobacco (Han et al., 2016) and sorghum (Chang et al., 2016), their functions in pearl millet are unclear. In order to characterize the SBP genes in pearl millet (*PgSBP*s), we analyzed the SBP genes in the pearl millet genome and performed phylogenetic analysis, conserved domain analysis, and the *cis*-element analysis for these genes. Expression patterns of *PgSBP*s, *PgmiR156*, and *PgmiR529* under various conditions were also investigated. The results can help to perform further functional analysis of *PgSBP*s in pearl millet.

2. Materials and methods

2.1. Plant materials

One inbred pearl millet line, ICMB 843, which had been evaluated as a drought-tolerant line in the International Crop Research Institute of Semi-Arid Tropics (ICRISAT), India, was used in this study. Seeds were sown in the soil that consists of akadama (80%), vermiculite (10%), charcoal (8%), slow-release (1%), and quick-release (1%) fertilizers. Plants were grown in a greenhouse in Tokyo, Japan, under the sunlight in July and August (with the day length of 13.5–14.5 h and the maximum light intensity ~1300 $\mu mol \cdot m^{-2} \cdot s^{-1}$). The temperature and relative humidity in the greenhouse were set for 25 °C and 65%, respectively. These settings kept the actual temperature 25–28 °C and the actual humidity 55–75%. For gene cloning, root samples were collected from 4-week-old plants, while for expression analysis, roots and leaves were collected from 4-week-old untreated plants (Control) and plants treated with 15% (*w/v*) PEG6000, 250 mM NaCl, 42 °C and 25 μM abscisic acid (ABA) for 6 h and 24 h.

2.2. Identification and bioinformatic analysis of PgSBPs

In a previous study, the whole genome of pearl millet was sequenced, and individual gene and protein sequences were deduced from this whole genome sequence (Varshney et al., 2017). These protein sequences were submitted as the query to the HMMER hmmscan program to identify *ab initio* the proteins with an SBP domain (Pfam accession number: PF03110). CD-search (https://www.ncbi.nlm.nih.gov/Structure/cdd/wrpsb.cgi) and Pfam (https://pfam.xfam.org/family/PF03110) were used to confirm the presence of the SBP domain in those proteins. Sequence logos for the SBP domain were generated by WebLogo 2.8.2 (http://weblogo.berkeley.edu/logo.cgi) (Crooks et al., 2004). The molecular weight (MW) and theoretical isoelectric point (pI) of PgSBPs were calculated using the ProtParam tool on the ExPASy server (https://web.expasy.org/protparam/). The conserved motifs were obtained by MEME 5.0.5 program (http://meme-suite.org/tools/meme) with the following parameters: a maximum number of motifs 16; motif width range 6–50 residues (Bailey et al., 2009). Intron/exon structures of *PgSBP*s were determined by aligning the cDNA sequences of *PgSBP*s to their corresponding genomic sequences using Gene Structure Display Server 2.0 (http://gsds.cbi.pku.edu.cn/index.php) (Hu et al., 2015). The *cis*-acting elements in the 2000 bp promoter regions were detected by the online website PlantCARE (http://bioinformatics.psb.ugent.be/webtools/plantcare/html/) (Lescot, 2002).

2.3. Chromosome location, the percentage identity matrix, and phylogenetic analysis

Chromosome locations of the *PgSBP*s were determined by the Map Gene 2 Chromosome v2 (http://mg2c.iask.in/mg2c_v2.0/). A percentage identity matrix of PgSBP was built on the basis of the sequence alignment using Clustal Omega (https://www.ebi.ac.uk/Tools/msa/clustalo/) and presented as a heatmap in HemI 1.0 (Deng et al., 2014). The SBP domain sequences of pearl millet, sorghum, rice, and foxtail millet were used together for the phylogenetic analysis. Multiple sequence alignment was conducted by ClustalW with default parameters in the MEGA X software. The phylogenetic tree was reconstructed by using the maximum-likelihood (ML) method with 1000 bootstrap replications based on the JTT + G model (Kumar et al., 2016). The resulting tree was visualized using iTOL v4 (Letunic and Bork, 2019).

2.4. Prediction of PgSBPs targeted by PgmiRNAs

The 290 microRNA sequences of pearl millet were obtained from previous small RNA sequencing data (Shinde et al., 2020). *PgSBP*s targeted by *PgmiR156q* or *PgmiR529b* were predicted by the psRNATarget server (http://plantgrn.noble.org/psRNATarget/) with default parameters (Dai et al., 2018b).

2.5. DNA isolation and PCR amplification

Genomic DNA was extracted from the roots of 4-week-old pearl millet plants with a DNeasy Plant Mini Kit (QIAGEN, Germany) in accordance with the manufacturer's instructions. *PgSBP* sequences were obtained by PCR using the genomic DNA as the template. Primers used for the PCR are listed in Table S1. The PCR products were gel-purified by FastGene Gel/PCR Extraction Kit (Genetics, Japan) and sequenced by Macrogen, Japan.

2.6. RNA extraction and quantitative reverse transcription-PCR (qRT-PCR) analysis

Total RNA was extracted from leaves and roots of the 4-week-old pearl millet plants with a NucleoSpin RNA Plant kit (MACHEREY-NAGEL, Germany) according to the manufacturer's instructions. cDNA was synthesized from 1 μg of the total RNA with Prime Script Reverse Transcriptase (Takara, Japan) and the oligo (dT) primer. The expression levels of *PgSBP*s were quantified by the quantitative reverse transcription-PCR (qRT-PCR), which was performed with the StepOne Real-Time PCR System (Applied Biosystems, USA) and the TB Green Premix Ex Taq™ (Takara, Japan). The PCR cycle was: 95 °C for 30 s, followed by 40 cycles at 95 °C for 5 s and 60 °C for 30 s, and then a dissociation curve analysis was performed at 95 °C for 60 s, 55 °C for 30 s, and 95 °C for 30 s. The *Ubiquitin* (*UBQ*) gene (GenBank accession number XM_004977046.2) (Anup et al., 2017) was used as the reference gene. Gene-specific primers for the *PgSBP*s were designed by the Primer-BLAST online server (https://www.ncbi.nlm.nih.gov/tools/primer-blast/) based on the MIQE guidelines (http://rdml.org/miqe). The primers are listed in Supplementary Table S2. The comparative Ct method was used to quantify expression levels (Schmittgen and Livak, 2008). For microRNA expression analysis, the cDNA was reverse-transcribed from 2 μg of the total RNA with the Mir-XTM miRNA First-Strand Synthesis Kit (Takara, Japan). For the qRT-PCR, the entire sequences of mature microRNAs were used for forward primers, and the mRQ3' primer from the kit was used as the reverse primer. U6 snRNA from the kit was used as the reference RNA. The PCR was conducted as described above.

Table 1
The 18 *PgSBP*s identified in pearl millet and their sequence characteristics.

Name	Gene ID	Gene length (bp)	CDS length (bp)	No. of amino acids (aa)	MW	pI
PgSBP1	MW561430	12,237	2568	855	94.01	5.59
PgSBP2	MW561431	2966	1314	437	45.84	6.75
PgSBP3	MW561432	2994	858	285	31.10	9.72
PgSBP4	MW561433	3467	1482	493	52.46	9.14
PgSBP5	MW561434	2546	1164	387	39.23	9.58
PgSBP6	MW561435	3153	1191	396	43.16	7.47
PgSBP7	MW561436	4390	858	285	30.30	8.33
PgSBP8	MW561437	2463	1296	431	45.84	9.24
PgSBP9	MW561438	3027	1302	433	47.42	8.95
PgSBP10	MW561439	2082	846	281	29.98	9.34
PgSBP11	MW561440	4262	2424	807	90.07	6.78
PgSBP12	MW561441	2995	540	179	19.03	10.19
PgSBP13	MW561442	2947	501	166	17.41	9.98
PgSBP14	MW561443	3625	774	257	27.73	10.28
PgSBP15	MW561444	4231	2964	987	10.89	5.96
PgSBP16	MW561445	5312	2934	977	10.67	5.54
PgSBP17	MW561446	2670	864	287	30.41	8.95
PgSBP18	MW561447	3245	966	322	34.01	6.56

3. Results

3.1. Identification, molecular cloning, and gene feature analysis of *PgSBP*s

Eighteen SBP genes (*PgSBP1–18*) were identified in the pearl millet genome and their sequences were deposited in the NCBI database (Table 1). The lengths of these genomic sequences varied from 2082 bp (*PgSBP10*) to 12,237 bp (*PgSBP1*). The coding sequences of *PgSBP*s ranged from 501 bp (*PgSBP13*) to 2964 bp (*PgSBP15*), with the deduced proteins ranging from 166 to 987 amino acids in length and from 10.67 (PgSBP16) to 94.01 (PgSBP1) kDa in protein mass. The predicted pI of the PgSBPs varied from 5.54 (PgSBP16) to 10.28 (PgSBP14). Among all the PgSBPs, 12 members are basic proteins with pI values more than 7.0 and the rest are acidic proteins (Table 1). PgSBPs in general have low identities to each other, except that PgSBP7 and PgSBP13 share 66% identity, PgSBP7 and PgSBP14 share 62% identity, and PgSBP13 and PgSBP17 share 62% identity (Fig. S1 and Table S3). Fourteen *PgSBP*s (*PgSBP1–14*) were unevenly distributed on 7 chromosomes with one gene on Chr1 and Chr4; two on Chr3, Chr5, and Chr6; and three on Chr2 and Chr7 (Fig. 1). *PgSBP15*, *PgSBP16*, *PgSBP17,* and *PgSBP18* were located on scaffolds (i.e., genomic sequences that have not been assigned to any chromosome) 2013, 2474, 2484, and 4011, respectively.

3.2. Sequence alignments and phylogenetic analysis of SBP domains

SBP domains have high similarity with each other and most of the PgSBPs have both Zn-1 and Zn-2 as well as an NLS in their SBP domains (Fig. 2). However, PgSBP7, PgSBP10, PgSBP14, and PgSBP18 lack Zn-1 and a part of Zn-2 (Fig. 2A). PgSBP11, PgSBP15, and PgSBP16 contain not only a SBP domain but also an ankyrin (ANK) domain (Fig. S2), which is associated with protein-protein interactions (Michaely and Bennett, 1992).

A phylogenetic tree was constructed using the highly conserved SBP-domains of the 18 PgSBPs, 27 *Setaria italica* SBP proteins (SiSBPs), 39 *Sorghum bicolor* SBP proteins (SbSBPs), and 19 *Oryza sativa* SBP proteins (OsSBPs). The resulting tree suggests that the 18 PgSBPs can be classified into seven groups (group I to VII, Fig. 3) and that all of these groups contain at least one SBP member from each species. Group VII is the largest group with six PgSBPs included. Groups I and II are the smallest groups with only one PgSBP member included.

3.3. Structural organization and conserved motif analysis of *PgSBP*s

Intron/exon structures of the 18 *PgSBP*s were analyzed by their genomic sequences and protein-coding sequences. The number of exons among *PgSBP*s ranged from 2 (*PgSBP12* and *PgSBP13*) to 11 (*PgSBP16*). The *PgSBP*s in the same group in the phylogenetic tree shared a similar intron/exon structure (Fig. 4).

In addition to the SBP and ANK domains, 16 motifs were identified for the 18 PgSBPs (Fig. 5, Table S5). The number of these motifs in each PgSBPs varies from 1 (PgSBP3) to 10 (PgSBP11 and PgSBP16) and the proteins in group IV possess the largest numbers of conserved motifs. Motif 1, motif 2, and motif 3 represent the N terminal, C terminal, and middle parts of the SBP domain, respectively. Some of these motifs are

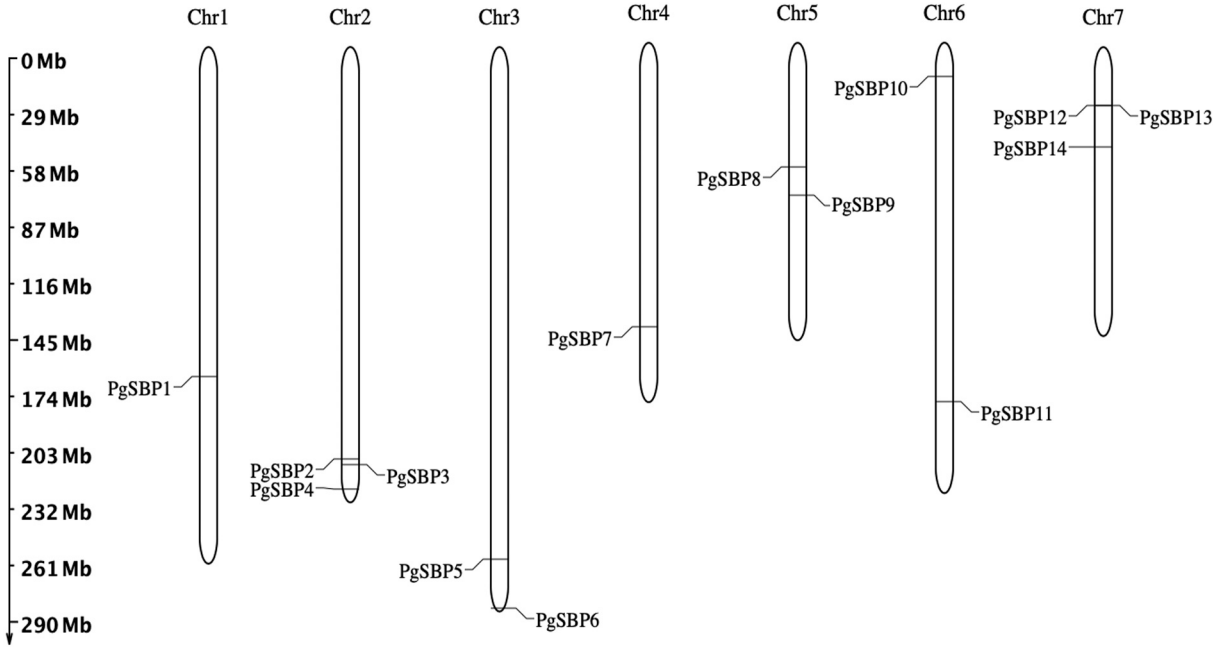

Fig. 1. Positions of SBP genes in pearl millet chromosomes. The chromosome number is indicated at the top of each bar (i.e., chromosome). The scale is represented in mega base (Mb).

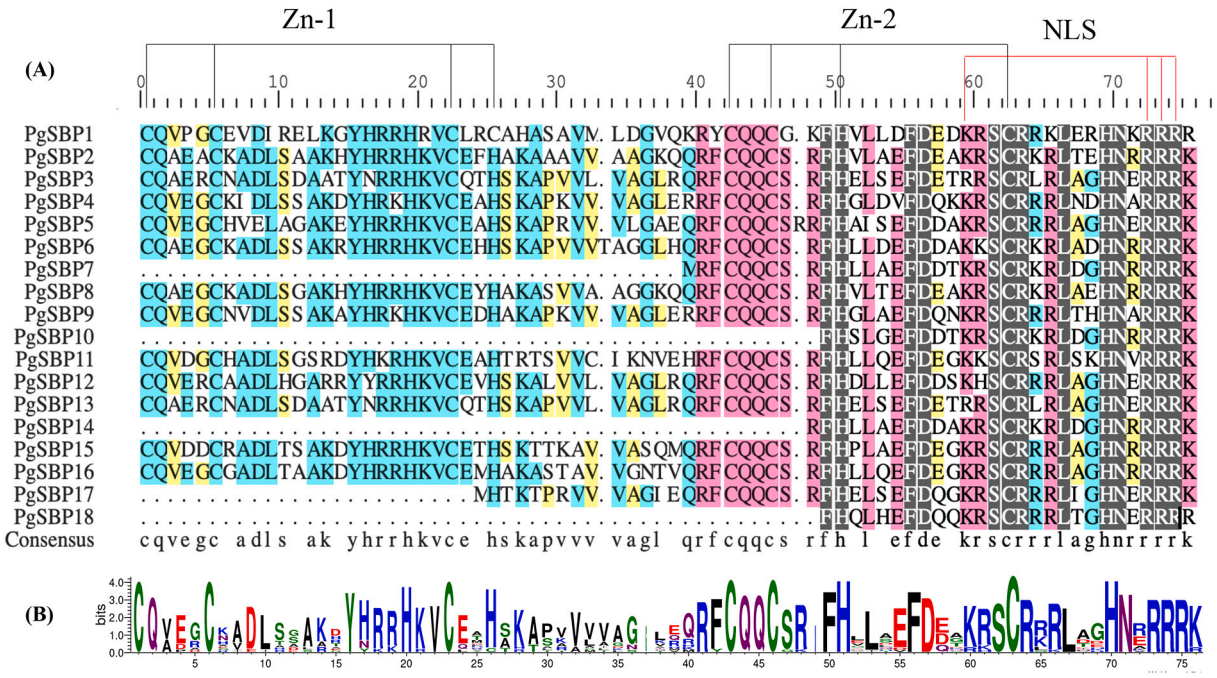

Fig. 2. Alignment of PgSBPs. (A) Multiple alignment of SBP domains of PgSBPs obtained with DNAMAN software. The two conserved zinc-finger structures (Zn-1 and Zn-2) and NLSs are indicated. (B) Sequence logos for the SBP domain of PgSBPs. The overall height of each stack represents the extent of conservation at each position, while the height of the letters within each stack indicates the relative frequency of the corresponding amino acid.

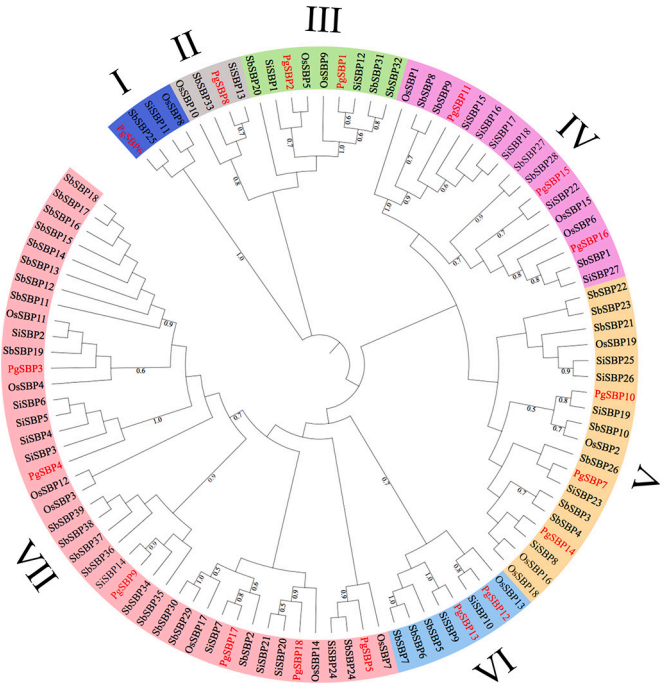

Fig. 3. The maximum likelihood (ML) phylogenetic tree of SBP proteins from pearl millet (PgSBP), sorghum (SbSBP), foxtail millet (SiSBP) and rice (OsSBP). The SBP domain sequences of all genes used for phylogenetic tree construction are listed in Supplementary Table S4.

specific to some groups. These data support the idea that the PgSBPs in the same group have similar functions.

3.4. Cis-elements analysis in the promoter regions of PgSBPs

The *cis*-elements in the 2000-bp promoter regions of *PgSBP*s were identified (Table S6) and were categorized into six groups based on the predicted functions shown in Fig. 6. The *cis*-elements identified include the elements regulating hormone responsiveness, such as the ABA-responsive elements (ABREs), the methyl jasmonate (MeJA)-responsive elements (CGTCA-motifs), auxin-responsive elements (TGA-elements and AuxRR-core elements), salicylic acid (SA)-responsive elements (TCA-element and SARE) and GA-responsive elements (GARE motifs, P-boxes, and TATC-boxes) (Table S6). Stress-associated *cis*-elements were also identified, such as the low-temperature responsive elements (LTREs), the drought-responsive elements (DREs), the MYB binding sites (MBSs), and TC-rich repeats. All the *PgSBP*s except *PgSBP3* and *PgSBP18* have some of those *cis*-elements, raising the possibility that most of the *PgSBP*s are either induced or repressed by phytohormones and/or abiotic stresses.

3.5. The regulation of the PgSBPs transcript by PgmiR156q and PgmiR529b

Nine out of the 18 *PgSBP*s (*PgSBP3*, *PgSBP4*, *PgSBP5*, *PgSBP7*, *PgSBP9*, *PgSBP10*, *PgSBP14*, *PgSBP17*, and *PgSBP18*), which encode PgSBPs in the groups V and VII, were found to be potential targets of a pearl millet *miR156*, *PgmiR156q* (Fig. 7A). All these genes, except *PgSBP4,* are also potential targets of a pearl millet *miR529*, *PgmiR529b* (Fig. S3). The distances between their SBP domain-coding sequences and putative microRNA binding sites were similar between these *PgSBP*s (326 bp–418 bp) (Fig. 7B). These results raise the possibility that these microRNA target sites originated from the common ancestor.

3.6. Expression profiles of PgSBPs, PgmiR156q, and PgmiR529b in different tissues under various abiotic stresses

In order to explore the possible functions of *PgSBP*s, the expression profiles of all *PgSBP*s were investigated in root and leaf tissues under salinity-stressed, drought-stressed, heat-stressed, and ABA-supplemented conditions with qRT-PCR (Fig. 8). In leaf tissues, two genes, *PgSBP8* and *PgSBP10*, were upregulated by salinity stress and *PgSBP2* was upregulated by drought stress. Twelve out of 18 *PgSBP*s

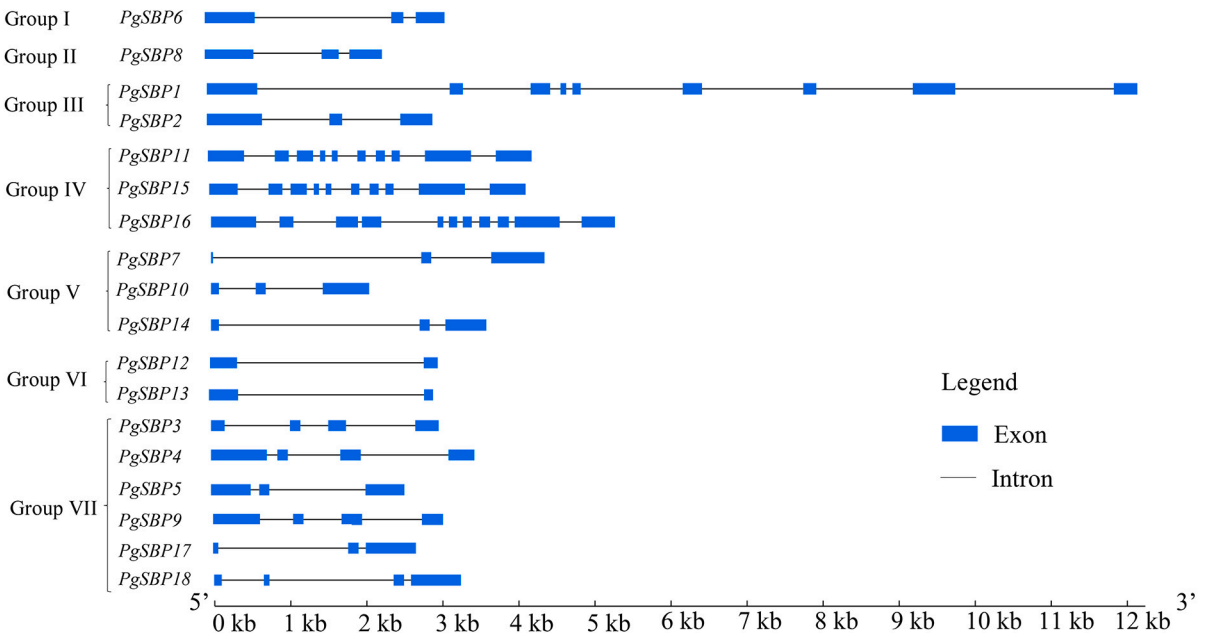

Fig. 4. Exon/intron structures of *PgSBP*s. Exons and introns are indicated by blue rectangles and black horizontal lines, respectively. (For interpretation of the references to colour in this figure legend, the reader is referred to the web version of this article.)

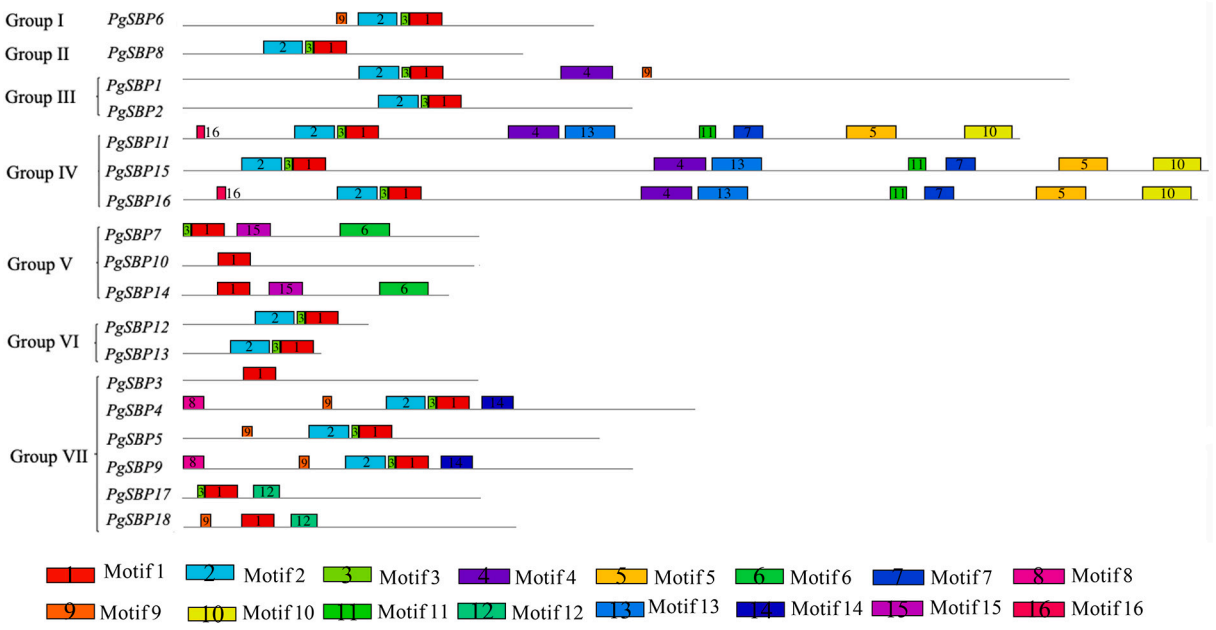

Fig. 5. Distribution of conversed motifs in PgSBPs. Motifs indicated by boxes were detected by MEME and the number in boxes (1 to 16) represents motif 1 to motif 16, respectively. Box sizes indicate the length of the motifs and the consensus sequences of these motifs are presented in Table S5.

were upregulated by heat stress. In roots, most of the *PgSBP*s were upregulated by salinity, drought, and heat stresses. According to previous RNA sequencing data (Dudhate et al., 2018), the absolute expression levels of *PgSBP3*, *PgSBP10*, *PgSBP11*, *PgSBP15*, and *PgSBP16* were higher than the other *PgSBP*s in root tissues under a control condition (Fig. S4). All these 5 *PgSBP*s were significantly induced by salinity, drought, and heat stresses (Fig. 8). The expression of *PgSBP2* in roots was 205 and 119 times stronger in the presence of salinity and drought stresses, respectively, compared to expression in control roots. The expression of *PgSBP7* and *PgSBP13* in roots was also 109 times stronger in the presence of salinity stress than in control roots (Fig. 8). Thus, although the absolute expression levels of these genes in roots are low (Fig. S4), they may regulate salinity and/or drought stress responsiveness. Further studies are necessary to clarify their functions.

Expression of pearl millet *miR156* and *miR529* (*PgmiR156q* and *PgmiR529b*) was also examined under the same conditions. In general, the expression patterns of *PgmiR156q* and *PgmiR529b* were similar to each other and opposite to *PgSBP*s (Fig. 8). For instance, *PgmiR156q* and *PgmiR529b* were downregulated in roots by the salinity and drought stresses, which upregulated the *PgmiR156q*- and *PgmiR529b*- targeted *PgSBP*s. These results support the idea that the expression levels of some of the *PgSBP*s are regulated by *PgmiR156q* and *PgmiR529b*.

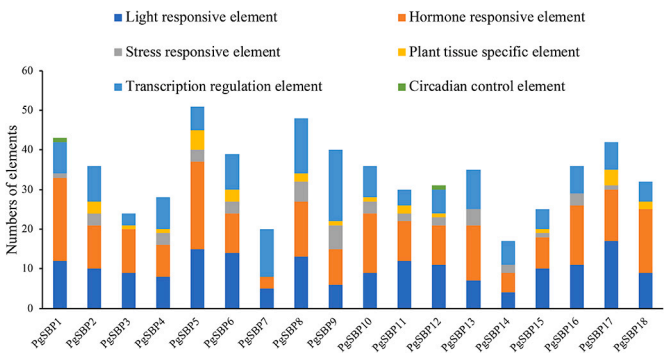

Fig. 6. *Cis*-elements in promoter regions of *PgSBPs*. The elements were identified from 2000 bp upstream promoter regions and the detailed information of these *cis*-elements is given in Table S6.

3.7. Expression profiles of PgSBPs, PgmiR156q, and PgmiR529b in different tissues under ABA treatment

Expression levels of the 18 *PgSBPs* were analyzed in roots and leaves treated with 25 μM ABA (Fig. 9). All of these *PgSBPs* were downregulated by a 24-h ABA treatment in leaf tissues and many of these genes were also downregulated by the same treatment in root tissues. In contrast, the expression levels of *PgmiR156q* and *PgmiR529b* were increased in both leaves and roots by the ABA treatment. These results suggest that ABA induces *PgmiR156q* and *PgmiR529b-PgSBPs* and thereby downregulates *PgSBPs*.

4. Discussion

In this study, 18 *PgSBPs* were identified in the pearl millet genome (Table 1). This number is similar to the numbers of *SBP*-like genes in *Arabidopsis thaliana* (16) (Cardon et al., 1999), *Betula luminifera* (18) (Lin et al., 2018), *Oryza sativa* (19) (Xie et al., 2006), *Camellia sinensis* (20) (Wang et al., 2018a), and *Carica papaya* (14) (Xu et al., 2020). However, the number is smaller than the numbers of SBP-like genes in *Setaria italica* (27) (Tian et al., 2017), *Zea mays* (31) (Mao et al., 2016), and *Glycine max* (41) (Tripathi et al., 2017). This may be because the *SBPs* evolved in a species-specific manner.

The 18 PgSBPs were divided into seven groups based on phylogenetic analysis (Fig. 3). This is consistent with the classification of SBPs of other species, such as cotton (Zhang et al., 2014), rice (Xie et al., 2006) and maize (Mao et al., 2016). PgSBPs in group IV have the ANK domain, which is predicted to promote a protein-protein interaction (Fig. S2). The ANK domain is also present in 6 SBPs in maize, 3 SBPs in luminifera, and 6 SBPs in cotton (Mao et al., 2016; Lin et al., 2018; Li and Lu, 2014). These findings suggest that the ANK domain is relevant to the functions of these SBPs.

Many of the 19 rice *SBPs* (*OsSPL1–19*, which correspond to *OsSBP1–19*, respectively, in Fig. 3) have been characterized. *OsSPL3* can be downregulated by *miR156* and *OsSPL3* induces the expression of the *WRKY71* transcription factor gene, thereby negatively regulating cold stress tolerance (Zhou and Tang, 2019). *OsSPL3* and *OsSPL12* are also known as positive regulators of crown root development (Shao et al., 2019). *OsSPL6* represses the expression of an endoplasmic reticulum stress sensor gene, *OsIRE1*, thereby regulating panicle development (Wang et al., 2018b). *OsSPL7* can also be downregulated by *miR156* and *OsSPL7* directly regulates the expression of the auxin-related gene *OsGH3.8*, thereby decreasing the tiller number (Dai et al., 2018a). OsSPL8 regulates the development of ligules and auricles in leaves (Lee et al., 2007). *OsSPL9* is a positive regulator of copper transporter genes and can increase copper contents in shoots (Tang et al., 2016). OsSPL10 induces trichome initiation in leaves and glumes and decreases salt tolerance (Lan et al., 2019). *OsSPL13* can also be downregulated by *miR156* and increases cell sizes in the grain hull, thereby increasing grain length and yield (Si et al., 2016). OsSPL14 decreases the tiller number and increases stem strength, lodging resistance, grain number, and grain weight (Jiao et al., 2010; Miura et al., 2010). OsSPL16

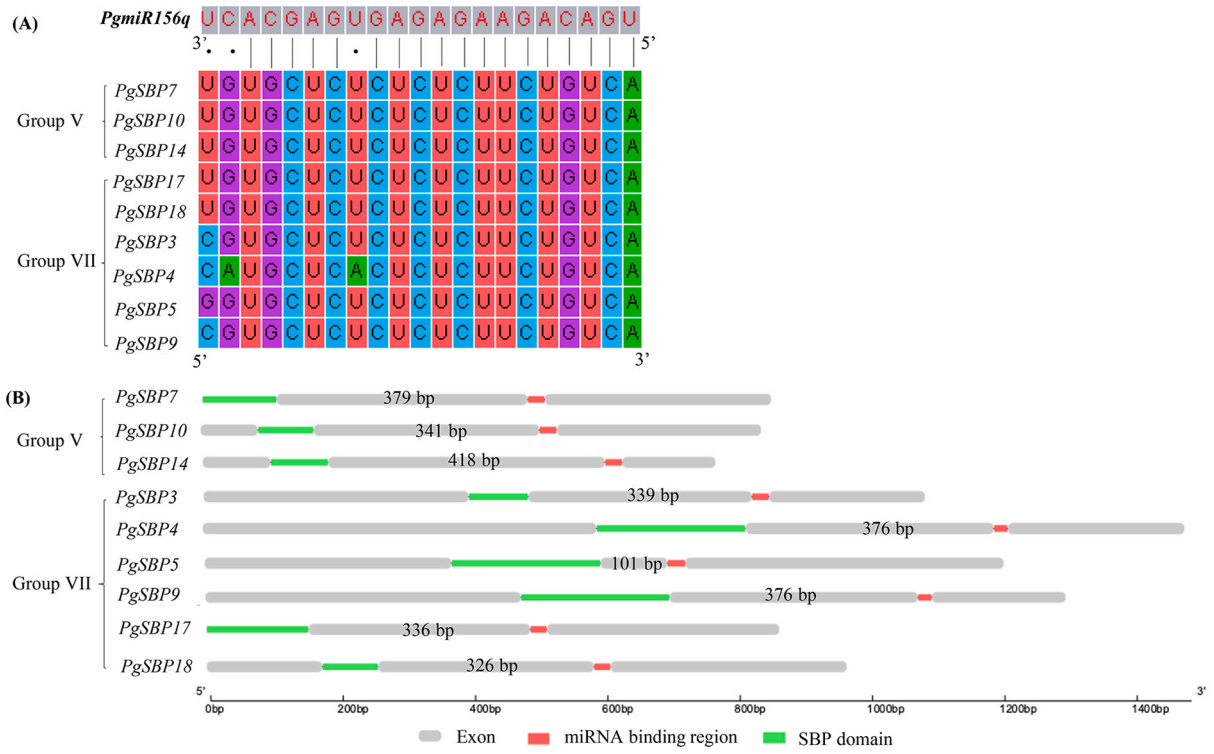

Fig. 7. *PgSBPs* targeted by *PgmiR156q*. (A) Alignment of the *PgmiR156q* mature sequence with complementary sequences of *PgSBPs*. The dots between miRNAs and targeted *PgSBP* sequences indicate mismatches. (B) The positions of miRNA binding regions and SBP domains in the sequences of *PgSBPs*.

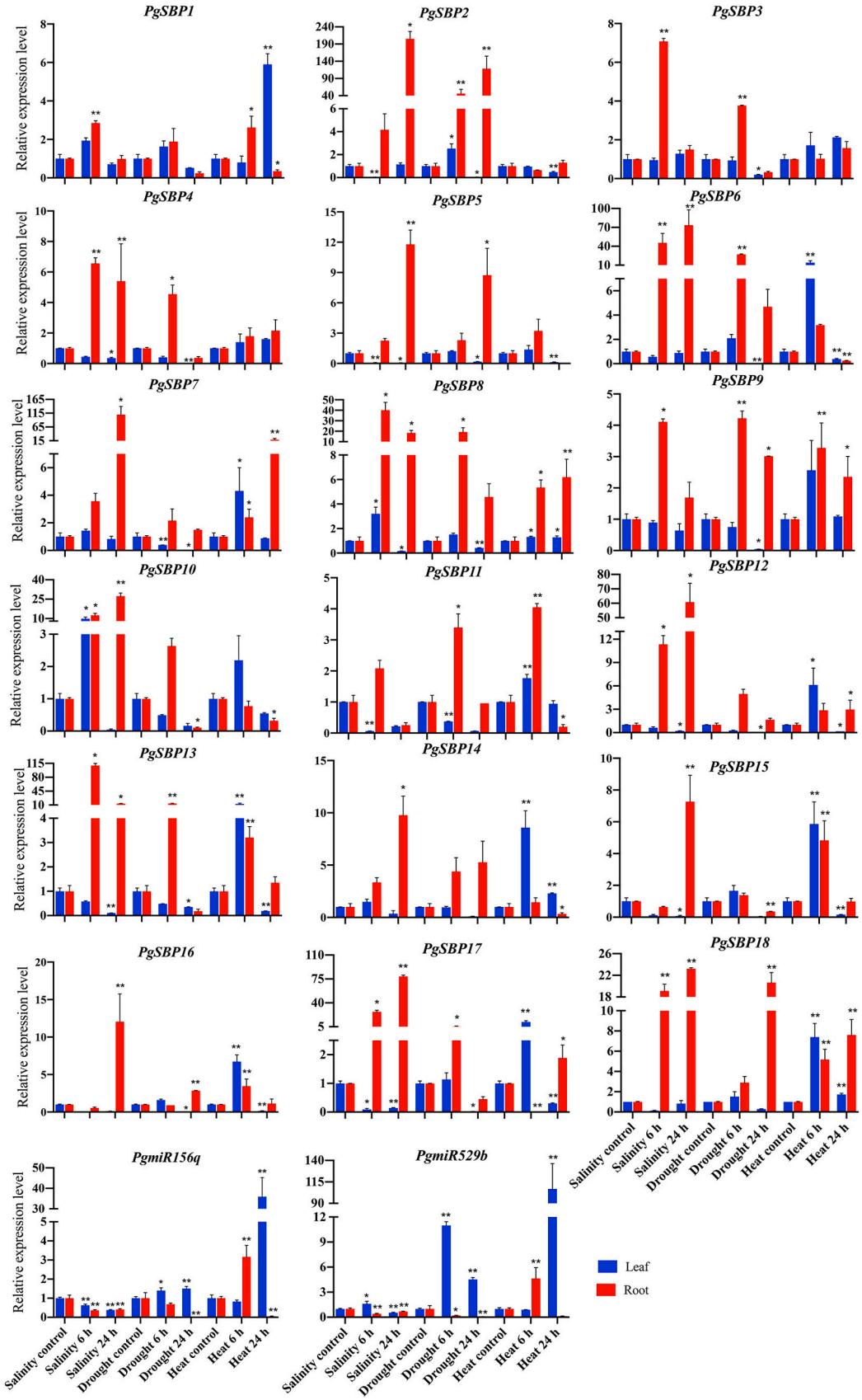

Fig. 8. The expression levels of *PgSBP*s, *PgmiR156q*, and *PgmiR529b* in leaves and roots in the presence of abiotic stresses. Four-week-old plants were treated with 250 mM NaCl (Salinity), 42 °C (Heat), and 15% (*W*/*V*) PEG6000 (Drought) for 6 h and 24 h. The expression levels were calculated by the $2^{-\Delta\Delta Ct}$ method. Asterisks indicate significant differences from each control. * $P < 0.05$, ** $P < 0.01$, Student's *t*-test.

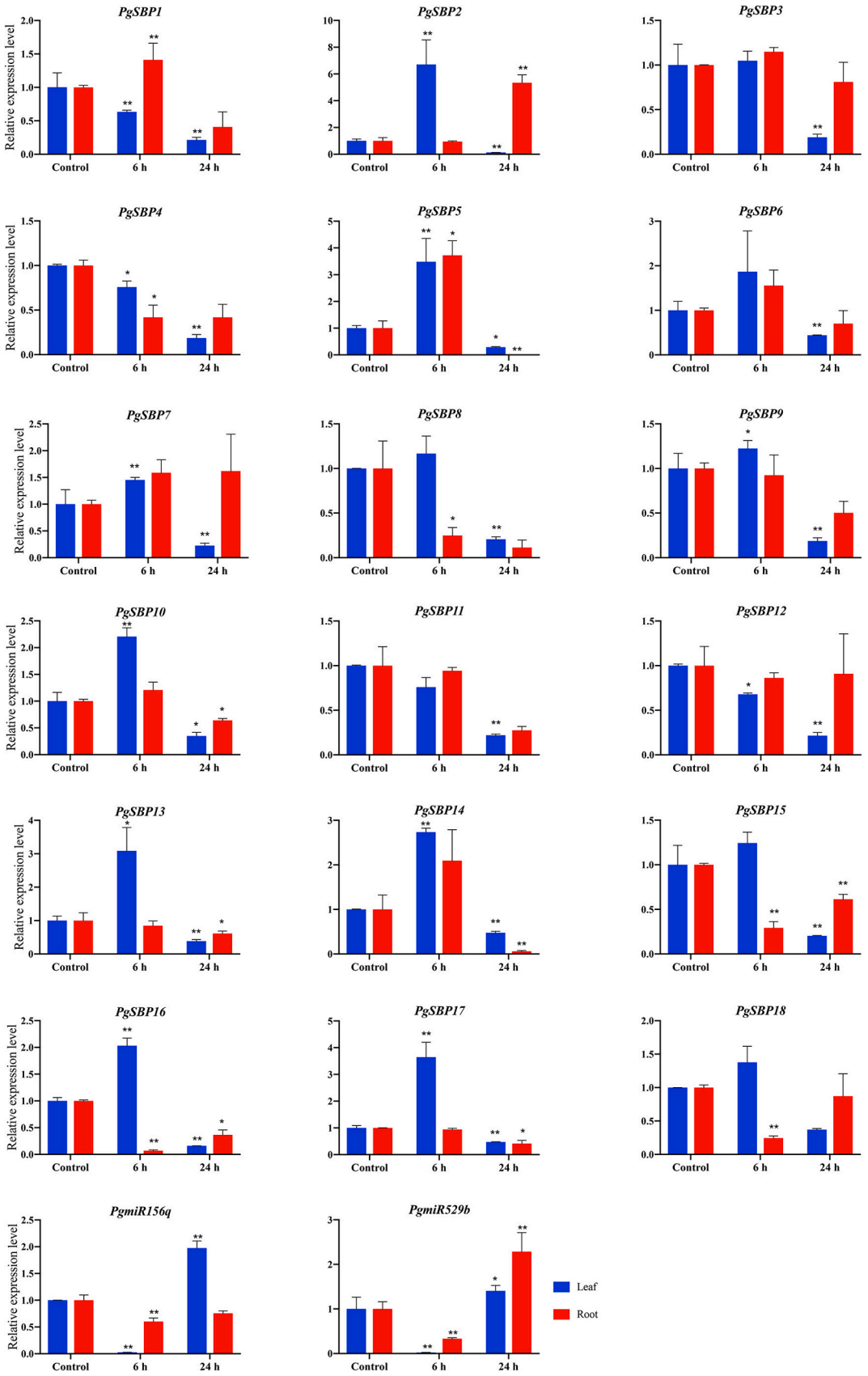

Fig. 9. The expression level of *PgSBP*s, *PgmiR156q*, and *PgmiR529b* in leaves and roots in the presence of ABA. Four-week-old plants were treated with 25 μM ABA for 6 h and 24 h. The expression levels were calculated by the $2^{-\Delta\Delta Ct}$ method. Asterisks indicate significant differences from each control. $^{*}P < 0.05$, $^{**}P < 0.01$, Student's *t*-test.

promotes cell proliferation in grains, thereby increasing grain width and yield (Wang et al., 2012). *OsSPL14* and *OsSPL16* as well as their close homolog *OsSPL2* are downregulated by *miR156* (Xie et al., 2006) and *miR529* (Yue et al., 2017). *OsSPL18* can also be downregulated by *miR156*, and OsSPL18 increases panicle length, grain thickness, the grain number yet decreases the tiller number (Yuan et al., 2019). Our data suggest that pearl millet has close homologs of all of these rice SBP genes (Fig. 3). Physiological functions of SBP are likely to be conserved in pearl millet and rice, but the functions of the pearl millet SBPs need to be characterized in detail in the future.

Some SBP genes in other species play roles in regulating plant responses to abiotic stresses and phytohormones. For instance, overexpression of an *SBP* gene (*VpSBP16*) from a Chinese wild *Vitis* species in Arabidopsis enhances the tolerance to salinity and drought stresses (Hou et al., 2018). Several SBPs in *Betula luminifera* interact with two DELLA proteins and regulate GA responses (Lin et al., 2018). The overexpression of a *B. luminifera SBP*, *BpSPL9*, enhances tolerance to drought and salinity by scavenging reactive oxygen species (ROS) in *B. platyphylla* Suk (Ning et al., 2017). Some of the 14 SBP genes in papaya (*Carica papaya*) are induced at a specific stage in fruit ripening and this process can be controlled by the phytohormone ethylene (Xu et al., 2020). *TaSPL14*, a close *OsSPL14* homolog in wheat (*Triticum aestivum*), does not regulate the tiller number but binds to the promoters of the ethylene-related genes *TaEIL1*, *TaRAP2.11*, and *TaERF1* and increases their expression, thereby regulating plant height, panicle length, the spikelet number, and grain weight (Cao et al., 2021). In this study, ABA-responsive elements and stress-responsive elements were found in most of the *PgSBP* promoters and ABA treatments reduced the expression levels of these genes. In addition, the expression levels of most *PgSBP*s in roots were increased by various abiotic stresses. Therefore, we hypothesize that PgSBPs play essential roles in pearl millet responses to abiotic stresses and phytohormones.

Supplementary data to this article can be found online at https://doi.org/10.1016/j.plgene.2021.100313.

Funding

This work was supported by JSPS KAKENHI Grant Number JP19H02928.

Declaration of Competing Interest

The authors declare no conflict of interest.

Acknowledgements

We are grateful to ICRISAT, India for providing the pearl millet seeds for this study. Pei Yu also thanks financial support by the China Scholarship Council (CSC).

References

Anup, P.C., Melvin, P., Kini, K.R., 2017. Reference gene selection and validation for gene expression studies in downy mildew infected pearl millet by quantitative real-time PCR. Australas. Plant Pathol. 46, 441–452. https://doi.org/10.1007/s13313-017-0506-z.

Arshad, M., Feyissa, B.A., Amyot, L., Aung, B., Hannoufa, A., 2017. MicroRNA156 improves drought stress tolerance in alfalfa (*Medicago sativa*) by silencing *SPL13*. Plant Sci. 258, 122–136. https://doi.org/10.1016/j.plantsci.2017.01.018.

Bailey, T.L., Boden, M., Buske, F.A., Frith, M., Grant, C.E., Clementi, L., Ren, J., Li, W.W., Noble, W.S., 2009. MEME suite: tools for motif discovery and searching. Nucleic Acids Res. 37, 202–208. https://doi.org/10.1093/nar/gkp335.

Bennetzen, J.L., Schmutz, J., Wang, H., Percifield, R., Hawkins, J., Pontaroli, A.C., Estep, M., Feng, L., Vaughn, J.N., Grimwood, J., Jenkins, J., Barry, K., Lindquist, E., Hellsten, U., Deshpande, S., Wang, X., Wu, X., Mitros, T., Triplett, J., Yang, X., Ye, C.-Y., Mauro-Herrera, M., Wang, L., Li, P., Sharma, M., Sharma, R., Ronald, P.C., Panaud, O., Kellogg, E.A., Brutnell, T.P., Doust, A.N., Tuskan, G.A., Rokhsar, D., Devos, K.M., 2012. Reference genome sequence of the model plant Setaria. Nat. Biotechnol. 30, 555–561. https://doi.org/10.1038/nbt.2196.

Chang, J., Yan, F., Qiao, L., Zheng, J., Zhang, F., Liu, Q., 2016. Genome-wide identification and expression analysis of SBP-box gene family in *Sorghum bicolor* L. Yi chuan = Hered 38, 569–580. https://doi.org/10.16288/j.yczz.16-008.

Cao, J., Liu, K., Song, W., Zhang, J., Yao, Y., Xin, M., Hu, Z., Peng, H., Ni, Z., Sun, Q., Du, J., 2021. Pleiotropic function of the *SQUAMOSA* PROMOTER-BINDING PROTEIN-LIKE gene *TaSPL14* in wheat plant architecture. Planta 253, 1–12. https://doi.org/10.1007/s00425-020-03531-x.

Cardon, G., Höhmann, S., Klein, J., Nettesheim, K., Saedler, H., Huijser, P., 1999. Molecular characterisation of the Arabidopsis SBP-box genes. Gene 237, 91–104. https://doi.org/10.1016/S0378-1119(99)00308-X.

Chen, K., Rajewsky, N., 2007. The evolution of gene regulation by transcription factors and microRNAs. Nat. Rev. Genet. 8, 93–103. https://doi.org/10.1038/nrg1990.

Chen, X., 2009. Small RNAs and their roles in plant development. Annu. Rev. Cell Dev. Biol. 25, 21–44. https://doi.org/10.1146/annurev.cellbio.042308.113417.

Crooks, G., Hon, G., Chandonia, J., Brenner, S., 2004. NCBI GenBank FTP Site \nWebLogo: a sequence logo generator. Genome Res. 14, 1188–1190. https://doi.org/10.1101/gr.849004.1.

Cui, L.G., Shan, J.X., Shi, M., Gao, J.P., Lin, H.X., 2014. The *miR156-SPL9-DFR* pathway coordinates the relationship between development and abiotic stress tolerance in plants. Plant J. 80, 1108–1117. https://doi.org/10.1111/tpj.12712.

Dai, X., Zhuang, Z., Zhao, P.X., 2018b. PsRNATarget: a plant small RNA target analysis server (2017 release). Nucleic Acids Res. 46, W49–W54. https://doi.org/10.1093/nar/gky316.

Dai, Z., Wang, J., Yang, X., Lu, H., Miao, X., Shi, Z., 2018a. Modulation of plant architecture by the *miR156f-OsSPL7-OsGH3.8* pathway in rice. J. Exp. Bot. 69, 5117–5130. https://doi.org/10.1093/jxb/ery273.

Deng, W., Wang, Y., Liu, Z., Cheng, H., Xue, Y., 2014. HemI: a toolkit for illustrating heatmaps. PLoS One 9, e1119888. https://doi.org/10.1371/journal.pone.0111988.

Dudhate, A., Shinde, H., Tsugama, D., Liu, S., Takano, T., 2018. Transcriptomic analysis reveals the differentially expressed genes and pathways involved in drought tolerance in pearl millet [*pennisetum glaucum* (l.) r. Br]. PLoS One 13, e0195908. https://doi.org/10.1371/journal.pone.0195908.

Gou, J., Fu, C., Liu, S., Tang, C., Debnath, S., Flanagan, A., Ge, Y., Tang, Y., Jiang, Q., Larson, P.R., Wen, J., Wang, Z.Y., 2017. The *miR156-SPL4* module predominantly regulates aerial axillary bud formation and controls shoot architecture. New Phytol. 829–840. https://doi.org/10.1111/nph.14758.

Gou, J.Y., Felippes, F.F., Liu, C.J., Weigel, D., Wang, J.W., 2011. Negative regulation of anthocyanin biosynthesis in *Arabidopsis* by a miR156-targeted SPL transcription factor. Plant Cell 23, 1512–1522. https://doi.org/10.1105/tpc.111.084525.

Han, Y.Y., Ma, Y.Q., Li, D.Z., Yao, J.W., Xu, Z.Q., 2016. Characterization and phylogenetic analysis of fifteen *NtabSPL* genes in *Nicotiana tabacum* L. cv. Qinyan95. Dev. Genes Evol. 226, 1–14. https://doi.org/10.1007/s00427-015-0522-3.

Hou, H., Jia, H., Yan, Q., Wang, X., 2018. Overexpression of a SBP-box gene (*VpSBP16*) from chinese wild *vitis* species in Arabidopsis improves salinity and drought stress tolerance. Int. J. Mol. Sci. 19, 940. https://doi.org/10.3390/ijms19040940.

Hu, B., Jin, J., Guo, A.Y., Zhang, H., Luo, J., Gao, G., 2015. GSDS 2.0: an upgraded gene feature visualization server. Bioinformatics 31, 1296–1297. https://doi.org/10.1093/bioinformatics/btu817.

Jiao, Y., Wang, Y., Xue, D., Wang, J., Yan, M., Liu, G., Dong, G., Zeng, D., Lu, Z., Zhu, X., Qian, Q., Li, J., 2010. Regulation of *OsSPL14* by *OsmiR156* defines ideal plant architecture in rice. Nat. Genet. 42, 541–544. https://doi.org/10.1038/ng.591.

Klein, J., Saedler, H., Huijser, P., 1996. A new family of DNA binding proteins includes putative transcriptional regulators of the *Antirrhinum majus* floral meristem identity gene *SQUAMOSA*. MGG Mol. Gen. Genet. 250, 7–16. https://doi.org/10.1007/s004380050046.

Kumar, S., Stecher, G., Tamura, K., 2016. MEGA7: molecular evolutionary genetics analysisversion 7.0 for bigger datasets. Mol. Biol. Evol. 33, 1870–1874. https://doi.org/10.1093/molbev/msw054.

Lan, T., Zheng, Y., Su, Z., Yu, S., Song, H., Zheng, X., Lin, G., Wu, W., 2019. *OsSPL10*, a SBP-box gene, plays a dual role in salt tolerance and trichome formation in rice (*Oryza sativa* L.). G3 Genes Genomes Genet. 9, 4107–4114. https://doi.org/10.1534/g3.119.400700.

Lee, J., Park, J.J., Kim, S.L., Yim, J., An, G., 2007. Mutations in the rice liguleless gene result in a complete loss of the auricle, ligule, and laminar joint. Plant Mol. Biol. 65, 487–499. https://doi.org/10.1007/s11103-007-9196-1.

Lescot, M., 2002. PlantCARE, a database of plant cis-acting regulatory elements and a portal to tools for in silico analysis of promoter sequences. Nucleic Acids Res. 30, 325–327. https://doi.org/10.1093/nar/30.1.325.

Letunic, I., Bork, P., 2019. Interactive tree of life (iTOL) v4: recent updates and new developments. Nucleic Acids Res. 47, W256–W259. https://doi.org/10.1093/nar/gkz239.

Li, C., Lu, S., 2014. Molecular characterization of the SPL gene family in *Populus trichocarpa*. BMC Plant Biol. 14, 131. https://doi.org/10.1186/1471-2229-14-131.

Lin, E.P., Niu, M.Y., Huang, H.H., Li, X.Y., Zhang, J.H., Tong, Z.K., 2018. Molecular characterization of *SQUAMOSA PROMOTER BINDING PROTEIN-LIKE* (*SPL*) gene family in *Betula luminifera*. Front. Plant Sci. 9, 1–17. https://doi.org/10.3389/fpls.2018.00608.

Mao, H.D., Yu, L.J., Li, Z.J., Yan, Y., Han, R., Liu, H., Ma, M., 2016. Genome-wide analysis of the SPL family transcription factors and their responses to abiotic stresses in maize. Plant Gene 6, 1–12. https://doi.org/10.1016/j.plgene.2016.03.003.

Matthews, C., Arshad, M., Hannoufa, A., 2019. Alfalfa response to heat stress is modulated by *microRNA156*. Physiol. Plant. 165, 830–842. https://doi.org/10.1111/ppl.12787.

Michaely, P., Bennett, V., 1992. The ANK repeat: a ubiquitous motif involved in macromolecular recognition. Trends Cell Biol. 2, 127–129. https://doi.org/10.1016/0962-8924(92)90084-Z.

Miura, K., Ikeda, M., Matsubara, A., Song, X.J., Ito, M., Asano, K., Matsuoka, M., Kitano, H., Ashikari, M., 2010. *OsSPL14* promotes panicle branching and higher grain productivity in rice. Nat. Genet. 42, 545–549. https://doi.org/10.1038/ng.592.

Ning, K., Chen, S., Huang, H., Jiang, J., Yuan, H., Li, H., 2017. Molecular characterization and expression analysis of the SPL gene family with *BpSPL9* transgenic lines found to confer tolerance to abiotic stress in *Betula platyphylla* Suk. Plant Cell Tissue Organ Cult. 130, 469–481. https://doi.org/10.1007/s11240-017-1226-3.

Schmittgen, T.D., Livak, K.J., 2008. Analyzing real-time PCR data by the comparative CT method. Nat. Protoc. 3, 1101–1108. https://doi.org/10.1038/nprot.2008.73.

Shao, Y., Zhou, H.Z., Wu, Y., Zhang, H., Lin, J., Jiang, X., He, Q., Zhu, J., Li, Y., Yu, H., Mao, C., 2019. OsSPL3, an SBP-domain protein, regulates crown root development in rice. Plant Cell 31, 1257–1275. https://doi.org/10.1105/tpc.19.00038.

Shinde, H., Dudhate, A., Anand, L., Tsugama, D., Gupta, S.K., Liu, S., Takano, T., 2020. Small RNA sequencing reveals the role of pearl millet miRNAs and their targets in salinity stress responses. S. Afr. J. Bot. 132, 395–402. https://doi.org/10.1016/j.sajb.2020.06.011.

Si, L., Chen, J., Huang, X., Gong, H., Luo, J., Hou, Q., Zhou, T., Lu, T., Zhu, J., Shangguan, Y., Chen, E., Gong, C., Zhao, Q., Jing, Y., Zhao, Y., Li, Y., Cui, L., Fan, D., Lu, Y., Weng, Q., Wang, Y., Zhang, Q., Liu, K., Wei, X., An, K., An, G., Han, B., 2016. OsSPL13 controls grain size in cultivated rice. Nat. Genet. 48, 447–456. https://doi.org/10.1038/ng.3518.

Tang, M., Zhou, C., Meng, L., Mao, D., Peng, C., Zhu, Y., Huang, D., Tan, Z., Chen, C., Liu, C., Zhang, D., 2016. Overexpression of *OsSPL9* enhances accumulation of Cu in rice grain and improves its digestibility and metabolism. J. Genet. Genomics 43, 673–676. https://doi.org/10.1016/j.jgg.2016.09.004.

Tian, F., Yang, D.C., Meng, Y.Q., Kong, L., Luo, J.C., Gao, G., 2017. PlantTFDB 4.0: toward a central hub for transcription factors and regulatory interactions in plants. Nucleic Acids Res. 45 (D1), D1040–D1045. https://doi.org/10.1093/nar/gkw982.

Tripathi, R.K., Goel, R., Kumari, S., Dahuja, A., 2017. Genomic organization, phylogenetic comparison, and expression profiles of the SPL family genes and their regulation in soybean. Dev. Genes Evol. 227, 101–119. https://doi.org/10.1007/s00427-017-0574-7.

Varshney, R.K., Shi, C., Thudi, M., Mariac, C., Wallace, J., Qi, P., Zhang, H., Zhao, Y., Wang, X., Rathore, A., Srivastava, R.K., Chitikineni, A., Fan, G., Bajaj, P., Punnuri, S., Gupta, S.K., Wang, H., Jiang, Y., Couderc, M., Katta, M.A.V.S.K., Paudel, D.R., Mungra, K.D., Chen, W., Harris-Shultz, K.R., Garg, V., Desai, N., Doddamani, D., Kane, N.A., Conner, J.A., Ghatak, A., Chaturvedi, P., Subramaniam, S., Yadav, O.P., Berthouly-Salazar, C., Hamidou, F., Wang, Jianping, Liang, X., Clotault, J., Upadhyaya, H.D., Cubry, P., Rhoné, B., Gueye, M.C., Sunkar, R., Dupuy, C., Sparvoli, F., Cheng, S., Mahala, R.S., Singh, B., Yadav, R.S., Lyons, E., Datta, S.K., Hash, C.T., Devos, K.M., Buckler, E., Bennetzen, J.L., Paterson, A.H., Ozias-Akins, P., Grando, S., Wang, Jun, Mohapatra, T., Weckwerth, W., Reif, J.C., Liu, X., Vigouroux, Y., Xu, X., 2017. Pearl millet genome sequence provides a resource to improve agronomic traits in arid environments. Nat. Biotechnol. https://doi.org/10.1038/nbt.3943.

Wang, J.W., Czech, B., Weigel, D., 2009. miR156-regulated SPL transcription factors define an endogenous flowering pathway in *Arabidopsis thaliana*. Cell 138, 738–749. https://doi.org/10.1016/j.cell.2009.06.014.

Wang, P., Chen, D., Zheng, Y., Jin, S., Yang, J., Ye, N., 2018a. Identification and expression analyses of SBP-box genes reveal their involvement in abiotic stress and hormone response in tea plant (*Camellia sinensis*). Int. J. Mol. Sci. 19, 3404. https://doi.org/10.3390/ijms19113404.

Wang, Q.L., Sun, A.Z., Chen, S.T., Chen, L.S., Guo, F.Q., 2018b. SPL6 represses signalling outputs of ER stress in control of panicle cell death in rice. Nat. Plants 4, 280–288. https://doi.org/10.1038/s41477-018-0131-z.

Wang, S., Wu, K., Yuan, Q., Liu, X., Liu, Z., Lin, X., Zeng, R., Zhu, H., Dong, G., Qian, Q., Zhang, G., Fu, X., 2012. Control of grain size, shape and quality by *OsSPL16* in rice. Nat. Genet. 44, 950–954. https://doi.org/10.1038/ng.2327.

Xie, K., Wu, C., Xiong, L., 2006. Genomic organization, differential expression, and interaction of *SQUAMOSA* promoter-binding-like transcription factors and *microRNA156* in rice. Plant Physiol. 142, 280–293. https://doi.org/10.1104/pp.106.084475.

Xu, Y., Xu, H., Wall, M.M., Yang, J., 2020. Roles of transcription factor SQUAMOSA promoter binding protein-like gene family in papaya (*Carica papaya*) development and ripening. Genomics 112, 2734–2747. https://doi.org/10.1016/j.ygeno.2020.03.009.

Yamasaki, K., Kigawa, T., Inoue, M., Tateno, M., Yamasaki, T., Yabuki, T., Aoki, M., Seki, E., Matsuda, T., Nunokawa, E., Ishizuka, Y., Terada, T., Shirouzu, M., Osanai, T., Tanaka, A., Seki, M., Shinozaki, K., Yokoyama, S., 2004. A novel zinc-binding motif revealed by solution structures of DNA-binding domains of Arabidopsis SBP-family transcription factors. J. Mol. Biol. 337, 49–63. https://doi.org/10.1016/j.jmb.2004.01.015.

Yu, N., Niu, Q.W., Ng, K.H., Chua, N.H., 2015. The role of miR156/SPLs modules in Arabidopsis lateral root development. Plant J. 83, 673–685. https://doi.org/10.1111/tpj.12919.

Yu, S., Galvão, V.C., Zhang, Y.C., Horrer, D., Zhang, T.Q., Hao, Y.H., Feng, Y.Q., Wang, S., Schmid, M., Wang, J.W., 2012. Gibberellin regulates the *Arabidopsis* floral transition through miR156-targeted SQUAMOSA PROMOTER BINDING–LIKE transcription factors. Plant Cell 24, 3320–3332. https://doi.org/10.1105/tpc.112.101014.

Yuan, H., Qin, P., Hu, L., Zhan, S., Wang, S., Gao, P., Li, J., Jin, M., Xu, Z., Gao, Q., Du, A., Tu, B., Chen, W., Ma, B., Wang, Y., Li, S., 2019. *OsSPL18* controls grain weight and grain number in rice. J. Genet. Genomics 46, 41–51. https://doi.org/10.1016/j.jgg.2019.01.003.

Yue, E., Li, C., Li, Y., Liu, Z., Xu, J.H., 2017. MiR529a modulates panicle architecture through regulating *SQUAMOSA* PROMOTER BINDING-LIKE genes in rice (*Oryza sativa*). Plant Mol. Biol. 94, 469–480. https://doi.org/10.1007/s11103-017-0618-4.

Zhang, H.X., Jin, J.H., He, Y.M., Lu, B.Y., Li, D.W., Chai, W.G., Khan, A., Gong, Z.H., 2016. Genome-wide identification and analysis of the SBP-box family genes under phytophthora capsici stress in pepper (*Capsicum annuum* L.). Front. Plant Sci. 7, 1–14. https://doi.org/10.3389/fpls.2016.00504.

Zhang, S.D., Ling, L.Z., 2018. Diversification of *SQUANOSA* promoter binding protein-like (*SPL*) genes by changes of *miR156/529* binding sites in land plants. Plant Gene 14, 55–63. https://doi.org/10.1016/j.plgene.2018.04.007.

Zhang, X., Dou, L., Pang, C., Song, M., Wei, H., Fan, S., Wang, C., Yu, S., 2014. Genomic organization, differential expression, and functional analysis of the *SPL* gene family in *Gossypium hirsutum*. Mol. Gen. Genomics. 290, 115–126. https://doi.org/10.1007/s00438-014-0901-x.

Zhou, M., Tang, W., 2019. *MicroRNA156* amplifies transcription factor-associated cold stress tolerance in plant cells. Mol. Gen. Genomics. 294, 379–393. https://doi.org/10.1007/s00438-018-1516-4.